

# Chaotic Synchronization in Nearest-Neighbor Coupled Networks of 3D CNNs

H. Serrano-Guerrero<sup>1</sup>, C. Cruz-Hernández<sup>\*2</sup>, R.M. López-Gutiérrez<sup>3</sup>, L. Cardoza-Avendaño<sup>3</sup>, R.A. Chávez-Pérez<sup>2</sup>

<sup>1</sup> Centro de Ingeniería y Tecnología (CITEC), Valle de las Palmas  
Universidad Autónoma de Baja California (UABC)

Tijuana, B.C., México

<sup>2</sup> Departamento de Electrónica y Telecomunicaciones

Centro de Investigación Científica y de Educación Superior de Ensenada (CICESE)

Ensenada, B.C., México

\*ccruz@cicese.mx

<sup>3</sup> Facultad de Ingeniería, Arquitectura y Diseño

Universidad Autónoma de Baja California

Ensenada, B.C., México

## ABSTRACT

In this paper, a synchronization of Cellular Neural Networks (CNNs) in nearest-neighbor coupled arrays, is numerically studied. Synchronization of multiple chaotic CNNs is achieved by appealing to complex systems theory. In particular, we consider dynamical networks composed by 3D CNNs, as interconnected nodes, where the interactions in the networks are defined by coupling the first state of each node. Four cases of interest are considered: i) synchronization without chaotic master, ii) master-slave configuration (directed ring), iii) open ring configuration (a path), and iv) directed path configuration. In addition, an application to chaotic communication networks is given.

Keywords: Chaotic synchronization, nearest-neighbor coupled networks, cellular neural networks (CNNs), chaotic communications.

## RESUMEN

En este trabajo se estudia numéricamente la sincronización de redes neuronales (CNNs) en arreglos acoplados con arreglos cercanos. Usando la teoría de sistemas complejos se logra la sincronización de múltiples CNNs. En particular, consideramos redes dinámicas compuestas por 3D CNNs, como nodos de la red, donde las interacciones en las redes se definen por el acoplamiento del primer estado de cada nodo de red. Se consideran cuatro casos de interés: i) sincronización sin maestro caótico, ii) configuración maestro-esclavo (anillo dirigido), iii) configuración de anillo abierto (camino) y iv) configuración de camino dirigido. Además, se da una aplicación a redes de comunicación caótica.

## 1. Introduction

Generally, a *chaotic oscillator* is a nonlinear deterministic system that possesses complex similarity to random behavior, continuous broadband power spectrum, and sensitive dependence on initial conditions, see e.g. [1–5]. Synchronization of chaotic systems have been developed and thoroughly studied over the past two decades, see e.g. [6–17] and references therein. It is a topic of both theoretical and practical interests. Because of its applications in communications, cryptography, neural networks, etc. For example, in engineering, mainly in the design of chaotic secure/private communication systems, see e.g. [18–26].

On the other hand, a *complex dynamical network* can be defined as a set of interconnected nodes, each node is considered a basic element with behavior depending on the nature of the network. These classes of structures have been observed in computer sciences, economy, biology, physics, chemistry, engineering, and social sciences, see e.g. [27–29].

Nowadays, synchronization is required in complex dynamical networks with many coupled identical nodes. The scenario where the connected nodes have *chaotic behavior* is particularly interesting.

Synchronization in complex dynamical networks has direct applications in different fields, see e.g. [24, 30–47]. Some interesting studies on artificial neural networks are reported in [48, 49]. In particular, *Cellular Neural Networks (CNNs)* exhibit chaotic dynamics, and so on, synchronization of CNNs becomes an important area of study. For example, CNN has broad applications in image and video signal processing, robotic, and biological visions [50]. In addition, synchronization of CNNs in different arrangements is very interesting by its possible application for security communication of encrypted information in a network of multiple users. Chaos plays a fundamental roll in the storage and retrieval of information in artificial and natural neural networks. Chaos has been observed and studied in CNNs [51, 52], in particular, some works on chaotic networks synchronization of CNNs with different coupling topologies can be consulted in [24, 39, 40, 43, 44].

Promising results on chaotic synchronization of coupled 3D CNNs in irregular arrays has been shown in [50]. However, the synchronization in nearest-neighbor coupled networks has direct application to chaotic communication systems.

The main goal of this paper is to synchronize multiple chaotic 3D CNNs (as interconnected nodes), that conform nearest-neighbor dynamical networks. This goal is achieved by appealing to results from complex systems theory. We arrange the chaotic 3D CNNs in nearest-neighbor coupled arrays in four scenarios: without chaotic master node, as a directed ring, as an open ring (path), and as a directed path. Finally, we present an application to chaotic communication in directed path coupled networks.

The organization of this paper is as follows: In Section 2, we describe the 3D CNN mathematical model to be used as fundamental node to construct the nearest-neighbor coupled networks. In Section 3, a brief review on synchronization in complex dynamical networks is given. In Section 4, we show the design of nearest-neighbor dynamical networks constructed using interconnected 3D CNNs and the synchronization in such networks. In Section 5, an application to encrypted chaotic network communications is presented. Finally, some concluding remarks are given in Section 6.

## 2. 3D CNN as fundamental node to be used to construct networks

Consider the following three-dimensional (3D) continuous time CNN [52],

$$\begin{aligned} C_i \frac{dx_i}{dt} &= -\frac{1}{R_i} x_i + \sum_{j=1}^3 T_{ij} v_j + I_i, \\ v_i &= S_i(x_i), \quad i=1,2,3, \end{aligned} \quad (1)$$

where  $S_i$  is a monotone differentiable function which is bounded above and below.  $\mathbf{T} = (T_{ij})$  is a  $3 \times 3$  matrix, called *weighting matrix* or *connection matrix* describing the strength of connections among neurons and  $I_i$  is a constant vector. In [52] it has been shown that under certain conditions the model Equation 1 exhibits chaotic behavior. The simplified mathematical model of a 3D CNN to be used to construct the nearest-neighbor dynamical networks, is given by [52]:

$$\dot{\mathbf{x}} = -\mathbf{x} + \mathbf{T} \tanh(\mathbf{x}), \quad (2)$$

where  $\mathbf{x} \in \mathbb{R}^3$  is the state vector, and

$$\mathbf{T} = \begin{pmatrix} T_{11} & T_{12} & T_{13} \\ T_{21} & T_{22} & T_{23} \\ T_{31} & T_{32} & T_{33} \end{pmatrix}. \quad (3)$$

The values for weighting matrix Equation 3 are given by:  $T_{11} = 1.49$ ,  $T_{12} = 2$ ,  $T_{13} = 1$ ,  $T_{21} = -2$ ,  $T_{22} = 1.7$ ,  $T_{23} = 0$ ,  $T_{31} = 4$ ,  $T_{32} = -4$ , and  $T_{33} = 2$ . The 3D CNN model defined by Equations 2 and 3 generates a chaotic attractor, see Figure 1. where the chaotic attractor (double-scroll type) of the 3D CNN is projected onto the  $(x_1, x_2, x_3)$ -space, when we have used the initial conditions  $x_1(0) = 0.14$ ,  $x_2(0) = -0.5$ , and  $x_3(0) = 0.1$ .

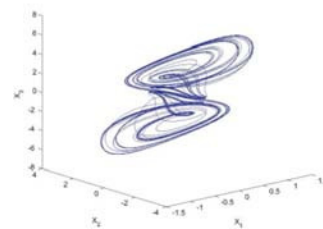


Figure 1. Chaotic attractor of 3D CNN projected onto the  $(x_1, x_2, x_3)$ -space.

Next, we show the arrangements for nearest-neighbor dynamical networks by using as coupled chaotic nodes to 3D CNNs defined by Equations 2 and 3.

### 3. Synchronization of complex dynamical networks

#### 3.1 Complex dynamical networks

We consider that complex dynamical networks are composed by  $N$  identical nodes, linear and diffusively coupled through the first state of each node. Each node constitutes a  $N$ -dimensional dynamical system, described as follows

$$\dot{\mathbf{x}}_i = \mathbf{f}(\mathbf{x}_i) + \mathbf{u}_i, \quad i = 1, 2, \dots, N, \quad (4)$$

where  $\mathbf{x}_i = (x_{i1}, x_{i2}, \dots, x_{iN})^T \in \mathbb{R}^N$  is the *state vector* of the node  $i$ ,  $\mathbf{u}_i \in \mathbb{R}^N$  is the *input* signal of the node  $i$ , and is defined by

$$\mathbf{u}_i = c \sum_{j=1}^N \mathbf{a}_{ij} \Gamma \mathbf{x}_j, \quad i = 1, 2, \dots, N, \quad (5)$$

the constant  $c > 0$  represents the *coupling strength*, and  $\Gamma \in \mathbb{R}^{N \times N}$  is a constant 0-1 matrix linking coupled states. Assume that  $\Gamma = \text{diag}(r_1, r_2, \dots, r_N)$  is a diagonal matrix with  $r_i = 1$  for a particular  $i$  and  $r_j = 0$  for  $j \neq i$ . This means that two coupled nodes are linked through their  $i$ -th state. Whereas,  $\mathbf{A} = (a_{ij}) \in \mathbb{R}^{N \times N}$  is the coupling matrix, which represents the coupling configuration in Equations 4 and 5. If there is a connection between node  $i$  and node  $j$ , then  $a_{ij} = 1$ ; otherwise,  $a_{ij} = 0$  for  $i \neq j$ . The diagonal elements of coupling matrix  $\mathbf{A}$  are defined as

$$a_{ii} = - \sum_{j=1, j \neq i}^N a_{ij} = - \sum_{j=1, j \neq i}^N a_{ji}, \quad i = 1, 2, \dots, N. \quad (6)$$

Let suppose that the dynamical network, Equations 4 and 5, is connected in the sense that there are no isolated clusters. Then, the coupling matrix  $\mathbf{A}$  is a symmetric irreducible matrix. In this case, zero is an eigenvalue of  $\mathbf{A}$  with multiplicity 1 and all the other eigenvalues are strictly negatives [45, 46]. Synchronization state in complex dynamical networks, Equations 4 and 5, can be characterized by the nonzero eigenvalues of the coupling matrix  $\mathbf{A}$ . The complex dynamical network, Equations 4

and 5, is said to achieve (asymptotically) *synchronization*, if [45]:

$$\mathbf{x}_1(t) = \mathbf{x}_2(t) = \dots = \mathbf{x}_N(t), \quad \text{as } t \rightarrow \infty. \quad (7)$$

The diffusive coupling condition in Equation 6 guarantees that the synchronization state is a solution,  $\mathbf{s}(t) \in \mathbb{R}^N$ , of an isolated node, that is

$$\dot{\mathbf{s}}(t) = \mathbf{f}(\mathbf{s}(t)), \quad (8)$$

where  $\mathbf{s}(t)$ , can be an equilibrium point, a periodic orbit or, a hyperchaotic attractor. Thus, stability of the synchronization state,

$$\mathbf{x}_1(t) = \mathbf{x}_2(t) = \dots = \mathbf{x}_N(t) = \mathbf{s}(t), \quad (9)$$

of complex networks in Equations 4 and 5, are determined by the dynamics of an isolated node, i.e. the nonlinear function  $\mathbf{f}$  (and its solution  $\mathbf{s}(t)$ ), the coupling strength  $c$ , the inner linking matrix  $\Gamma$ , and matrix  $\mathbf{A}$ . In this work we choose  $\Gamma = [1, 0, \dots, 0]$ , with this linking matrix, we can guarantee at least network synchronization of the first state of all nodes. Network synchronization among the first states of the nodes is enough to achieve the final goal of the chaotic synchronization that is the transmission of encrypted information. If we want to achieve network synchronization of all states of the nodes, then we should use all states of the nodes as signal timing, rather than just the first state.

#### 3.2 Synchronization conditions

**Theorem 1** [45, 46] *Consider the dynamical network in Equations 4 and 5. Let*

$$0 = \lambda_1 > \lambda_2 \geq \lambda_3 \geq \dots \geq \lambda_N \quad (10)$$

*be the eigenvalues of its coupling matrix  $\mathbf{A}$ . Suppose that there exists a  $N \times N$  diagonal matrix  $\mathbf{D} > 0$  and two constants  $\bar{d} < 0$  and  $\tau > 0$ , such that*

$$[\mathbf{D}\mathbf{f}(\mathbf{s}(t)) + \mathbf{d}\Gamma]^T \mathbf{D} + \mathbf{D}[\mathbf{D}\mathbf{f}(\mathbf{s}(t)) + \mathbf{d}\Gamma] \leq -\tau \mathbf{I}_N \quad (11)$$

*for all  $d \leq \bar{d}$ , where  $\mathbf{I}_N \in \mathbb{R}^{N \times N}$  is an unit matrix. If, moreover,*

$$c\lambda_2 \leq \bar{d}, \quad (12)$$

then, the synchronization state, Equation 9, of dynamical network in Equations 4 and 5 is exponentially stable.

Since  $\lambda_2 < 0$  and  $\bar{d} < 0$ , inequality in Equation 12 is equivalent to:

$$c \geq \left| \frac{\bar{d}}{\lambda_2} \right|. \quad (13)$$

Synchronizability of dynamical network in Equations 4 and 5 with respect to a specific coupling configuration can be characterized by the second-largest eigenvalue ( $\lambda_2$ ) of coupling matrix  $\mathbf{A}$ .

### 3.3 Nearest-neighbor coupled networks

The coupling configurations commonly studied in synchronization of complex dynamical networks are the so-called: globally coupled networks, nearest-neighbor coupled networks, and star coupled networks. In this work, we concentrate on the *synchronization in nearest-neighbor coupled networks with identical nodes (3D CNNs)*. In the sequel, we will show the particular arrangement of the coupling matrix for this class of complex dynamical networks. A nearest-neighbor coupled network consists of  $N$  nodes arranged in a ring, where each node  $i$  is adjacent to the neighbor nodes  $i \pm 1, i \pm 2, \dots, i \pm K/2$  where  $K$  is even, with coupling matrix defined by:

$$\mathbf{A} = \begin{pmatrix} -K & 1 & 0 & \dots & 1 \\ 1 & -K & 1 & \dots & 0 \\ \vdots & \ddots & \ddots & \ddots & \vdots \\ 0 & 0 & 1 & \dots & 1 \\ 1 & 0 & 0 & \dots & -K \end{pmatrix} \quad (14)$$

$$\begin{aligned} \dot{x}_{i1} &= -x_{i1} + T_{11} \tanh(x_{i1}) + T_{12} \tanh(x_{i2}) + T_{13} \tanh(x_{i3}) + u_{i1}, \\ \dot{x}_{i2} &= -x_{i2} + T_{21} \tanh(x_{i1}) + T_{22} \tanh(x_{i2}) + T_{23} \tanh(x_{i3}), \\ \dot{x}_{i3} &= -x_{i3} + T_{31} \tanh(x_{i1}) + T_{32} \tanh(x_{i2}) + T_{33} \tanh(x_{i3}), \end{aligned} \quad (15)$$

and the second largest eigenvalue given by:

$$\lambda_2 = -4 \sum_{j=1}^{K/2} \sin^2\left(\frac{j\pi}{N}\right).$$

For a fixed  $K$ ,  $\lambda_2$  decreases to zero as  $N$  goes to infinity

$$\lim_{N \rightarrow \infty} (\lambda_2) = 0, \quad (16)$$

condition in Equation 15 implies that the networks no synchronize if  $N$  is too large.

### 4. Synchronization of 3D CNNs in nearest-neighbor networks

In this section, first, we show the particular arrangements of nearest-neighbor dynamical networks, considering four coupling scenarios: nearest-neighbor networks without chaotic master, directed ring, open ring (path), and directed path, by using the 3D CNN-node (Equations 2 and 3) as fundamental node (see Figure 2). Finally, we show synchronization in the designed dynamical networks.

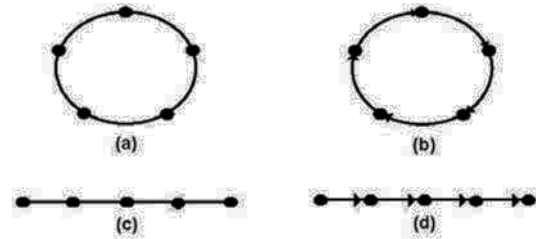


Figure 2 a) Nearest-neighbor coupled network, b) directed ring coupled network, c) open ring (path) coupled network, and d) directed path coupled network.

The complex dynamical networks to be constructed with  $N$  coupled 3D CNNs Equations 2 and 3, take the following form (according to Equations. 4 and 5),

for  $i = 1, 2, \dots, N$ , with input signals defined by

$$u_{i1} = c \sum_{j=1}^N a_{ij} x_{j1}. \quad (17)$$

If the input signals (Equation 17) are  $u_{i1} \equiv 0$  for  $i = 1, 2, \dots, N$ , then we have the original set of  $N$  uncoupled 3D CNNs (Equations 2 and 3), which evolve according to their own dynamics, and of course, the *uncoupled  $N$  nodes are not*

*synchronized*. In particular, for the networks in Equations 16 and 17, we consider  $N = 5$  and  $\Gamma = \text{diag}(1, 0, 0)$  from Equation 5, that is, we have five 3D CNN-nodes composing the (nearest-neighbor) dynamical networks to be synchronized.

Let us rewrite explicitly, the arrangements of the (nearest-neighbor) dynamical networks (Equations 16 and 17) for five nodes. The first 3D CNN-node is given by:

$$\begin{aligned} \dot{x}_{11} &= -x_{11} + T_{11} \tanh(x_{11}) + T_{12} \tanh(x_{12}) + T_{13} \tanh(x_{13}) + u_{11}, \\ \dot{x}_{12} &= -x_{12} + T_{21} \tanh(x_{11}) + T_{22} \tanh(x_{12}) + T_{23} \tanh(x_{13}), \\ \dot{x}_{13} &= -x_{13} + T_{31} \tanh(x_{11}) + T_{32} \tanh(x_{12}) + T_{33} \tanh(x_{13}), \\ u_{11} &= c(a_{11}x_{11} + a_{12}x_{21} + a_{13}x_{31} + a_{14}x_{41} + a_{15}x_{51}), \end{aligned} \quad (18)$$

the second one is described by

$$\begin{aligned} \dot{x}_{21} &= -x_{21} + T_{11} \tanh(x_{21}) + T_{12} \tanh(x_{22}) + T_{13} \tanh(x_{23}) + u_{21}, \\ \dot{x}_{22} &= -x_{22} + T_{21} \tanh(x_{21}) + T_{22} \tanh(x_{22}) + T_{23} \tanh(x_{23}), \\ \dot{x}_{23} &= -x_{23} + T_{31} \tanh(x_{21}) + T_{32} \tanh(x_{22}) + T_{33} \tanh(x_{23}), \\ u_{21} &= c(a_{21}x_{11} + a_{22}x_{21} + a_{23}x_{31} + a_{24}x_{41} + a_{25}x_{51}), \end{aligned} \quad (19)$$

the third one by means of

$$\begin{aligned} \dot{x}_{31} &= -x_{31} + T_{11} \tanh(x_{31}) + T_{12} \tanh(x_{32}) + T_{13} \tanh(x_{33}) + u_{31}, \\ \dot{x}_{32} &= -x_{32} + T_{21} \tanh(x_{31}) + T_{22} \tanh(x_{32}) + T_{23} \tanh(x_{33}), \\ \dot{x}_{33} &= -x_{33} + T_{31} \tanh(x_{31}) + T_{32} \tanh(x_{32}) + T_{33} \tanh(x_{33}), \\ u_{31} &= c(a_{31}x_{11} + a_{32}x_{21} + a_{33}x_{31} + a_{34}x_{41} + a_{35}x_{51}), \end{aligned} \quad (20)$$

the fourth one by

$$\begin{aligned} \dot{x}_{41} &= -x_{41} + T_{11} \tanh(x_{41}) + T_{12} \tanh(x_{42}) + T_{13} \tanh(x_{43}) + u_{41}, \\ \dot{x}_{42} &= -x_{42} + T_{21} \tanh(x_{41}) + T_{22} \tanh(x_{42}) + T_{23} \tanh(x_{43}), \\ \dot{x}_{43} &= -x_{43} + T_{31} \tanh(x_{41}) + T_{32} \tanh(x_{42}) + T_{33} \tanh(x_{43}), \\ u_{41} &= c(a_{41}x_{11} + a_{42}x_{21} + a_{43}x_{31} + a_{44}x_{41} + a_{45}x_{51}), \end{aligned} \quad (21)$$

and the fifth one as

$$\begin{aligned} \dot{x}_{51} &= -x_{51} + T_{11} \tanh(x_{51}) + T_{12} \tanh(x_{52}) + T_{13} \tanh(x_{53}) + u_{51}, \\ \dot{x}_{52} &= -x_{52} + T_{21} \tanh(x_{51}) + T_{22} \tanh(x_{52}) + T_{23} \tanh(x_{53}), \\ \dot{x}_{53} &= -x_{53} + T_{31} \tanh(x_{51}) + T_{32} \tanh(x_{52}) + T_{33} \tanh(x_{53}), \\ u_{51} &= c(a_{51}x_{11} + a_{52}x_{21} + a_{53}x_{31} + a_{54}x_{41} + a_{55}x_{51}), \end{aligned} \quad (22)$$

In the sequel, we present four nearest-neighbor connection topologies for networks with five 3D CNN-nodes, in the four cases: nearest-neighbor networks without chaotic master node, directed ring, open ring (path), and directed path.

**Case 1 (Network without master node):** Five uncoupled chaotic 3D CNN-nodes (Equations 2 and 3) to be synchronized in a dynamical network in a nearest-neighbor configuration without master node, see Figure 2(a).

The coupling matrix (Equation 14) for this case with  $K = 2$ , is given by

$$\mathbf{A} = \begin{pmatrix} -2 & 1 & 0 & 0 & 1 \\ 1 & -2 & 1 & 0 & 0 \\ 0 & 1 & -2 & 1 & 0 \\ 0 & 0 & 1 & -2 & 1 \\ 1 & 0 & 0 & 1 & -2 \end{pmatrix},$$

and the second largest eigenvalue is:

$$\lambda_2 = -4 \sum_{j=1}^{2/2} \sin^2\left(\frac{j\pi}{5}\right) = -1.382.$$

For synchronization purpose, we have designed the input signals  $u_{i1} = g(x_{i1}; c)$ ,  $i = 1, 2, \dots, 5$  to construct the mentioned arrangement, that explicitly are given by:

$$\begin{aligned} u_{11} &= c(-2x_{11} + x_{21} + x_{51}), \\ u_{21} &= c(x_{11} - 2x_{21} + x_{31}), \\ u_{31} &= c(x_{21} - 2x_{31} + x_{41}), \\ u_{41} &= c(x_{31} - 2x_{41} + x_{51}), \\ u_{51} &= c(x_{11} + x_{41} - 2x_{51}). \end{aligned} \quad (23)$$

To construct the nearest-neighbor coupled network without master node shown in Figure 2(a), we use Equations 18 and 22, with input signals from Equation 23. We take the initial conditions:  $x_{11}(0) =$

$0.14$ ,  $x_{12}(0) = 0.5$ ,  $x_{13}(0) = 0.1$ ,  $x_{21}(0) = 0.15$ ,  $x_{22}(0) = 0.6$ ,  $x_{23}(0) = 0.2$ ,  $x_{31}(0) = 0.16$ ,  $x_{32}(0) = 0.7$ ,  $x_{33}(0) = 0.05$ ,  $x_{41}(0) = 0.13$ ,  $x_{42}(0) = 0.4$ ,  $x_{43}(0) = 0.25$ ,  $x_{51}(0) = 0.12$ ,  $x_{52}(0) = 0.45$ , and  $x_{53}(0) = 0.3$ . With  $d = -1$  we can stabilize to zero all the states of a single (isolated) node. With  $\bar{d} = -1$ , we can obtain from Equation 13,  $c \geq 0.7236$ , for the computer simulations we have used the coupling value  $c = 70$ . With these values the Theorem 1 guarantees synchronization in the network with five chaotic 3D CNN-nodes. Figure 3, shows chaos synchronization in the first state of five 3D CNN-nodes,  $x_{i1}$ ,  $i = 1, \dots, 5$ , and the chaotic attractor corresponding to new chaotic collective behavior in the dynamical network (Equations 18 to 22) with input signals (Equation 23), projected onto the  $(x_{11}, x_{12}, x_{13})$ -space. Figures 4 and 5, show the phase diagrams of the second and third states, from these figures we can see that the second and third states do not synchronize.

**Case 2 (Directed ring):** Five uncoupled chaotic 3D CNN-nodes (Equations. 2 and 3) to be synchronized in a nearest-neighbor network with directed ring configuration, see Figure 2(b).

To construct the proposed arrangement, we have used the coupling signals  $x_{i1}$ ,  $i = 1, \dots, 5$  for the five 3D CNN-nodes. For this purpose, we have designed the input signals  $u_{i1} = g(x_{i1}; c)$ ,  $i = 1, \dots, 5$ , that explicitly are given by:

$$\begin{aligned} u_{11} &= c(-x_{11} + x_{51}), \\ u_{21} &= c(x_{11} - x_{21}), \\ u_{31} &= c(x_{21} - x_{31}), \\ u_{41} &= c(x_{31} - x_{41}), \\ u_{51} &= c(x_{41} - x_{51}). \end{aligned} \quad (24)$$

Now, by using Equations 18 to 22 with input signals (Equation 24) among chaotic 3D CNN-nodes, we have constructed the nearest-neighbor network with directed ring configuration shown in Figure 2(b) to be synchronized. For this network, the corresponding coupling matrix is given by

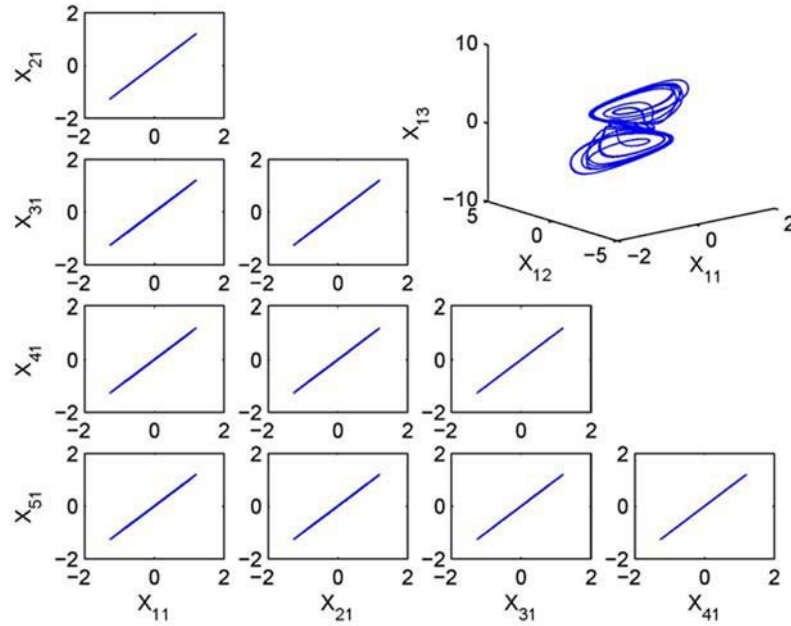


Figure 3. Synchronization in the first state ( $x_{i1}$ ,  $i = 1, \dots, 5$ ) of five chaotic 3D CNNs in nearest-neighbor configuration without master node, and the new chaotic attractor of the collective behavior, projected onto the  $(x_{11}, x_{12}, x_{13})$ -space.

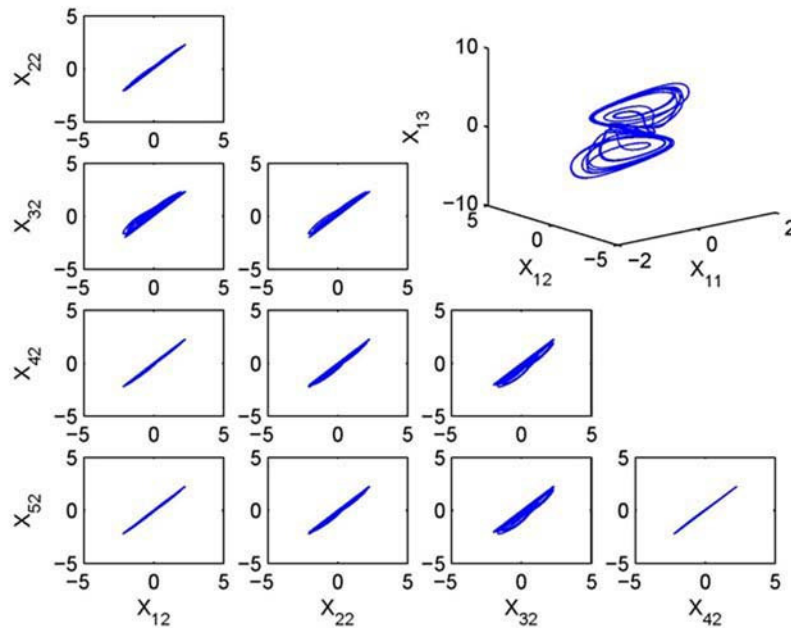


Figure 4. Phase diagrams of the second state ( $x_{i2}$ ,  $i = 1, \dots, 5$ ) of five chaotic 3D CNNs in nearest-neighbor configuration without master node, and the new chaotic attractor of the collective behavior in the network, projected onto the  $(x_{11}, x_{12}, x_{13})$ -space.

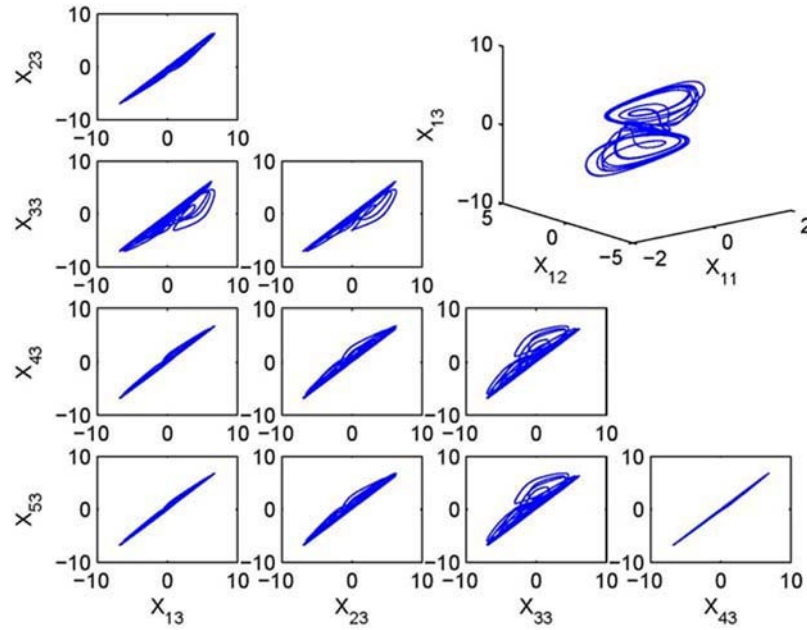


Figure 5. Phase diagrams of the third state ( $x_{i3}$ ,  $i = 1, \dots, 5$ ) of five chaotic 3D CNNs in nearest-neighbor configuration without master node, and the new chaotic attractor of the collective behavior in the network, projected onto the  $(x_{11}, x_{12}, x_{13})$ -space.

$$\mathbf{A} = \begin{pmatrix} -1 & 0 & 0 & 0 & 1 \\ 1 & -1 & 0 & 0 & 0 \\ 0 & 1 & -1 & 0 & 0 \\ 0 & 0 & 1 & -1 & 0 \\ 0 & 0 & 0 & 1 & -1 \end{pmatrix}$$

with eigenvalues:  $\lambda_1 = 0$ ,  $\lambda_2 = -0.691 + 0.9511j$ ,  $\lambda_3 = -0.691 - 0.9511j$ ,  $\lambda_4 = -1.809 + 0.5878j$ , and  $\lambda_5 = -1.809 - 0.5878j$ . Matrix  $\mathbf{A}$  is no longer symmetric, however their nonzero eigenvalues have negative real part, so Theorem 1 still holds. Initial conditions and the constants  $\bar{d}$  and  $d$  are the same as in previous case, and with coupling value  $c = 70$ . With these values the Theorem 1 guarantees chaos synchronization in the dynamical network with five 3D CNN-nodes. The Figure 6. shows chaos synchronization in the first state of five CNN-nodes, i.e.,  $x_{i1}$ ,  $i = 1, \dots, 5$ , and the chaotic attractor of the *collective behavior imposed by the master node 1* in the dynamical network, projected onto the  $(x_{11}, x_{12}, x_{13})$ -space.

**Case 3 (Open ring (path)):** Five uncoupled chaotic 3D CNN-nodes (Equations 2 and 3), to be synchronized in a nearest-neighbor network with open ring (path) configuration, see Figure 2(c). To construct the proposed arrangement, we have used the coupling signals  $x_{i1}$ ,  $i = 1, \dots, 5$  for the five 3D CNN-nodes. For this purpose, we have designed the input signals  $u_{i1} = g(x_{i1}; c)$ ,  $i = 1, \dots, 5$ , that explicitly are given by:

$$\begin{aligned} u_{11} &= c(-x_{11} + x_{21}), \\ u_{21} &= c(x_{11} - 2x_{21} + x_{31}), \\ u_{31} &= c(x_{21} - 2x_{31} + x_{41}), \\ u_{41} &= c(x_{31} - 2x_{41} + x_{51}), \\ u_{51} &= c(x_{41} - x_{51}). \end{aligned} \quad (25)$$

Now, by using Equations 18 to 22 with input signals (Equation 25) among chaotic 3D CNN-nodes, we have constructed the nearest-neighbor network with open ring (path) configuration, shown in Figure 2(c) to be synchronized. For this network, the corresponding coupling matrix is given by:



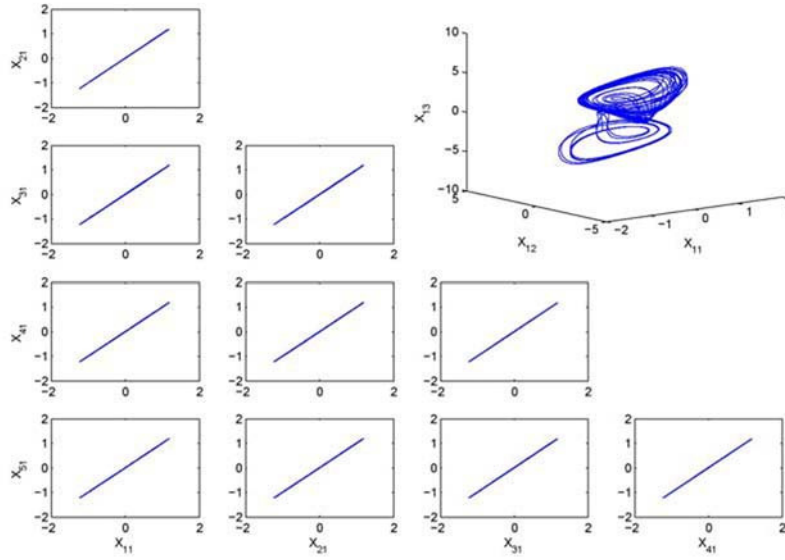


Figure 6. Synchronization in the first state ( $x_{i1}$ ,  $i = 1, \dots, 5$ ) of five chaotic 3D CNNs in nearest-neighbor network with directed node configuration, and the new chaotic attractor of the collective behavior in the network, projected onto the  $(x_{11}, x_{12}, x_{13})$ -space.

$$\mathbf{A} = \begin{pmatrix} -1 & 1 & 0 & 0 & 0 \\ 1 & -2 & 1 & 0 & 0 \\ 0 & 1 & -2 & 1 & 0 \\ 0 & 0 & 1 & -2 & 1 \\ 0 & 0 & 0 & 1 & -1 \end{pmatrix}$$

with eigenvalues:  $\lambda_1 = 0$ ,  $\lambda_2 = -0.382$ ,  $\lambda_3 = -1.382$ ,  $\lambda_4 = -2.618$ , and  $\lambda_5 = -3.618$ . Initial conditions and the constants  $\bar{d}$  and  $d$  are the same as in previous case, and with coupling value  $c = 70$ . With these values the Theorem 1 guarantees chaos synchronization in the dynamical network with five 3D CNN-nodes. Figure 7. shows chaos synchronization in the first state of five CNN-nodes, i.e.,  $x_{i1}$ ,  $i = 1, \dots, 5$ , and the chaotic attractor of the *collective behavior imposed by the master node 1* in the dynamical network, projected onto the  $(x_{11}, x_{12}, x_{13})$ -space.

**Case 4 (Directed path):** Five uncoupled chaotic 3D CNN-nodes (Equations 2 and 3,) to be synchronized in a nearest-neighbor network with directed path configuration, see Figure 2(d).

To construct the proposed arrangement, we have used the coupling signals  $x_{i1}$ ,  $i = 1, \dots, 5$  for the five 3D CNN-nodes. For this purpose, we have designed the input signals  $u_{i1} = g(x_{i1}; c)$ ,  $i = 1, \dots, 5$ , that explicitly are given by:

$$\begin{aligned} u_{11} &= 0, \\ u_{21} &= c(x_{11} - x_{21}), \\ u_{31} &= c(x_{21} - x_{31}), \\ u_{41} &= c(x_{31} - x_{41}), \\ u_{51} &= c(x_{41} - x_{51}). \end{aligned} \tag{26}$$

In this case,  $u_{11} = 0$  because the node 1 is the master node, i.e. it does not receive any input signal from any other node of the network; the role of the node 1 is to drive to other nodes. Now, by using Equations 18 to 22 with input signals (Equation 26) among chaotic 3D CNN-nodes, we have constructed the nearest-neighbor network with open ring (path) configuration, shown in Figure 2(d) to be synchronized. For this network, the corresponding coupling matrix is given by

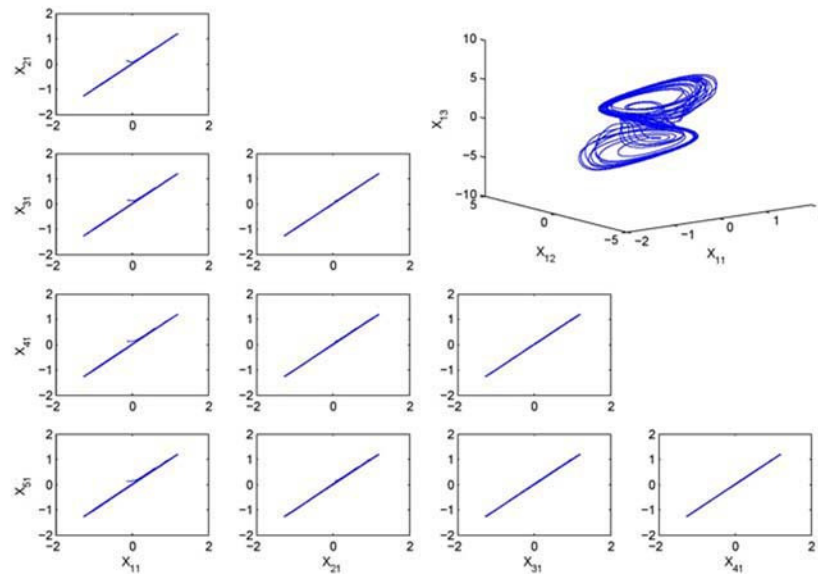


Figure 7. Synchronization in the first state ( $x_{i1}$ ,  $i = 1, \dots, 5$ ) of five chaotic 3D CNNs in nearest-neighbor network with open ring configuration, and the new chaotic attractor of the collective behavior in the network, projected onto the  $(x_{11}, x_{12}, x_{13})$ -space.

$$\mathbf{A} = \begin{pmatrix} 0 & 0 & 0 & 0 & 0 \\ 1 & -1 & 0 & 0 & 0 \\ 0 & 1 & -1 & 0 & 0 \\ 0 & 0 & 1 & -1 & 0 \\ 0 & 0 & 0 & 1 & -1 \end{pmatrix}$$

with eigenvalues:  $\lambda_1 = 0$ ,  $\lambda_2 = \lambda_3 = \lambda_4 = \lambda_5 = -1$ . Matrix  $\mathbf{A}$  is no longer symmetric, however their nonzero eigenvalues have negative real part, so Theorem 1 still holds. Initial conditions and the constants  $\bar{d}$  and  $d$  are the same as in previous case, and with coupling value  $c = 70$ . With these values the Theorem 1 guarantees chaos synchronization in the dynamical network with five 3D CNN-nodes. Figure 8, shows chaos synchronization in the first state of five CNN-nodes, i.e.,  $x_{i1}$ ,  $i = 1, \dots, 5$ , and the chaotic attractor of the *collective behavior imposed by the master node 1* in the dynamical network, projected onto the  $(x_{11}, x_{12}, x_{13})$ -space.

**Remark 1:** *It is important to mention that an exact synchronization was only achieved in the first state in the four cases (i.e., in second and third states, the synchronization is approximate, that is, the synchronization error is approximately to zero). Figures 4 and 5, show the phase diagrams of the second and third states for the first case of study. From these figures we can see that the second and third states do not synchronize. This behavior of the second and third states is repeated in the next three cases of study.*

## 5. Encrypted chaotic communications

In this final section, we apply the synchronization of five chaotic 3D CNNs with directed path configuration (Fig. 2(d)), to secure communication of confidential information. In particular, we construct a chaotic communication network system to transmit a encrypted pulse train as information. The purpose is to send the pulse train, from a transmitter (chaotic 3D CNN-node 1) to each receiver (3D CNN-nodes  $N_2$ ,  $N_3$ ,  $N_4$ , and  $N_5$ ) via public channels.

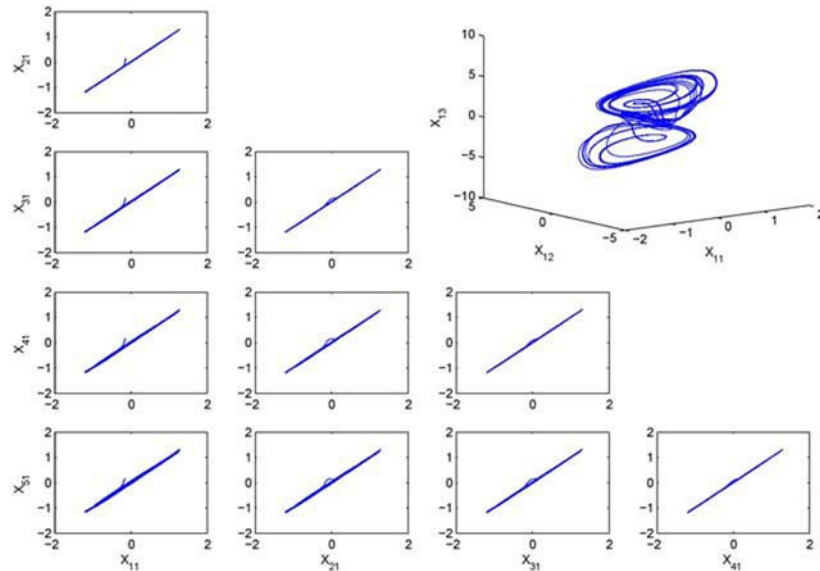


Figure 8. Synchronization in the first state ( $x_{i1}$ ,  $i = 1, \dots, 5$ ) of five chaotic 3D CNNs in directed path configuration, and the new chaotic attractor of the collective behavior in the network, projected onto the  $(x_{11}, x_{12}, x_{13})$ -space.

Figure 9. shows the chaotic communication scheme to transmit hidden messages from node  $N_1$  (transmitter) to the four remote receivers. The transmission is achieved by using chaotic switching technique, see e.g. [2, 4, 10-14]. In this technique, a binary signal  $m(t)$  is used to modulate one parameter of transmitter (node  $N_1$ ). According to the value of  $m(t)$  at any given time  $t$ , the transmitter has either the parameter value  $p$  or  $p'$ . For example, if is a '0' bit for transmission, then the transmitter has the parameter value  $p$ , otherwise the parameter value is  $p'$ . So,  $m(t)$  controls a switch whose action changes the parameter values between  $p$  and  $p'$  in the transmitter, while the remote receivers have all time the parameter value

$p$ . The synchronization error  $e_{i+1}(t) = x_{i,1}(t) - x_{i+1,1}(t)$ ,  $i = 1, 2, 3, 4$  decides if the received signal corresponds to a '0' or '1' bit. Thus, when transmitter and each receiver synchronize (i.e.,  $e_i(t) = 0$ ,  $i = 2, 3, 4, 5$ ) can be interpreted as a '0' bit, and when transmitter with the receivers no synchronize (i.e.,  $e_i(t) \neq 0$ ,  $i = 2, 3, 4, 5$ ) will be interpreted as a '1' bit. The difference between  $p$  and  $p'$  must be small so the transmitter node does not lose its chaotic behavior, but big enough to produce a momentaneous loss of synchrony with the other nodes of the network (receivers). This momentaneous loss of synchrony can be detected in the synchrony error. The correct value of  $p'$  is selected experimentally.

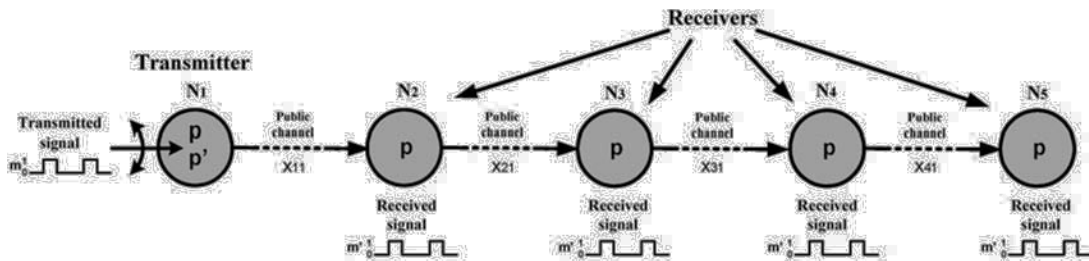


Figure 9 . Chaotic communication network system to transmit encrypted image messages.

In this work, to transmit an encrypted train pulse via chaotic switching, let  $T_{11}$  be the parameter to be modulated in the 3D CNN (Equation 18) node  $N_1$ . The binary information  $m(t)$  is added to  $T_{11}$  as follows,  $T_{11}(t) = T_{11} + r \cdot m(t)$ , where  $r = 0.01$ . Let us consider the train pulse shown in Figure 10(a) as the confidential message to be transmitted. In Figure 10(b), the first state of node  $N_1$  without transmission is shown. Figure 10(c) illustrates the train pulse transmission through an insecure channel in the communication network, when the parameter  $T_{11}$  in the transmitter (node  $N_1$ , Equation 18) is switched between  $T_{11} = 1.49$  (to encode a '0' bit) and  $T'_{11} = 1.5$  (to encode a '1' bit). At the remote receiver ends, the synchronization error

detection  $e_i(t) = x_{i,1}(m(t)) - x_{i+1,1}(t)$ ,  $i = 1, 2, 3, 4$  is achieved for the recovered binary sequence  $m'(t)$  after a low-pass filtering stage. Finally, from  $m(t)$ , the recovered train pulse message is shown in Figure 11. The rule to obtain the binary sequence  $m'(t)$  is based on the synchronization error detection  $e_i(t)$ ,  $i = 2, 3, 4, 5$  for each bit period to assign a '0' or '1' bit, as follows: when in the receiver ends we have  $e_i(t) \neq 0$ , then is a '1' bit and when  $e_i(t) = 0$ , then is a '0' bit. Note that, an eavesdropper (in any public channel of the communication network system) will obtain the encrypted image shown in Figure 10(c), constructed from the transmitted chaotic signal  $x_{11}(m(t))$ .

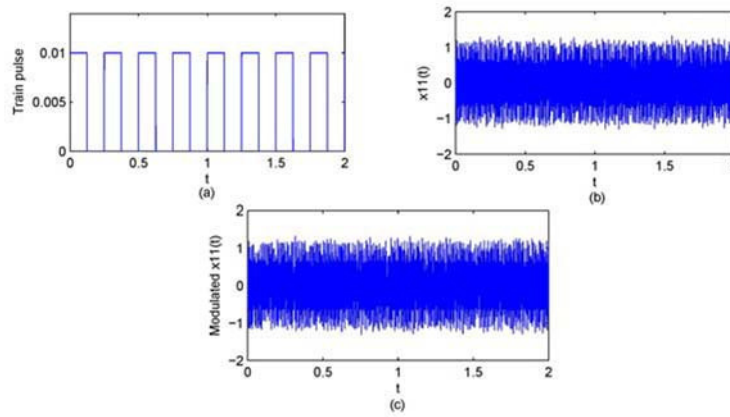


Figure 10 (a). Train pulse  $m(t)$  to be transmitted, (b) first state of the transmitter node  $N_1$  without transmission, (c) first state of the transmitter node  $N_1$  modulated with the message and transmitted through public channel.

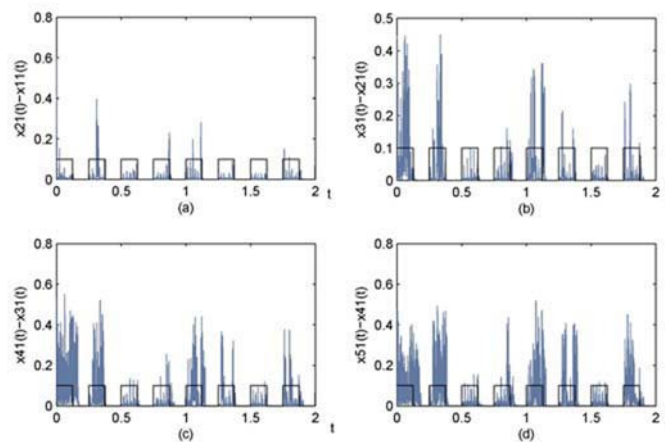


Figure 11. Synchronization error in each receiver node.



In the sequel, by using the same chaotic communication network system (see Figure 9), we illustrate the encrypted image transmission. Previously, in the encryption process, the image message is converted to a binary sequence, to obtain  $m$ . Figure 12 shows the image message to be sent to set of remote receivers, Figure 13, shows the chaotic encrypted image message, and Figure 14, the recovered image message from  $m'$  by the nodes  $N_2$ ,  $N_3$ ,  $N_4$ , and  $N_5$ . If we use a different node to transmit the message only the subsequent nodes will recover the message, in Table 1 a relation of this is shown. If we want to transmit a message to a prior node, we will need another directed path network in the opposite direction in order to have a full duplex connection.



Figure 12. Original image message ("mime") to be sent.

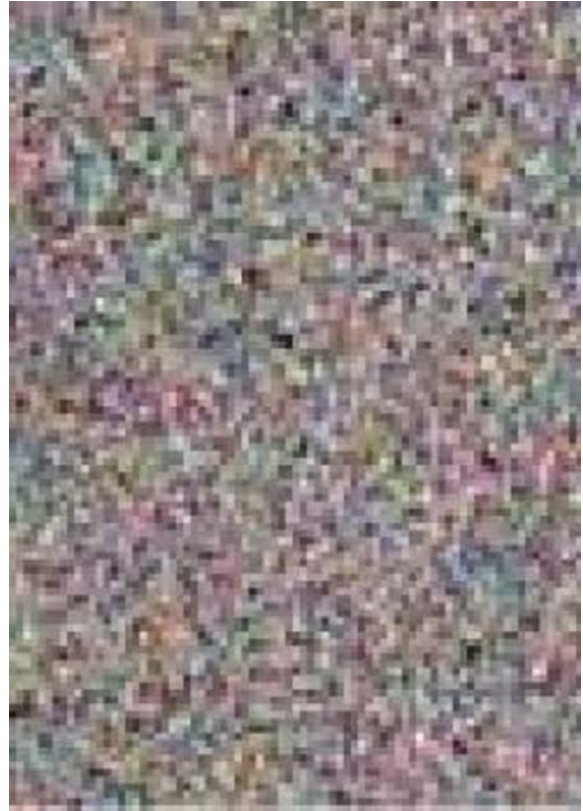


Figure 13 Chaotic encrypted image message through insecure channel.

## 6. Concluding remarks

In this paper, we have presented the synchronization of multiple coupled chaotic 3D CNNs. We have achieved synchronization in the designed of a nearest-neighbor complex networks in four scenarios, without chaotic master node, in a directed ring configuration, open ring (path) configuration and directed path configuration. It was shown that, in the three last presented cases, the synchronization in second and third states is only approximate, while the first state is synchronized, in the first scenario the synchronization is complete. In addition, based on synchronization of multiple 3D CNNs in nearest-neighbor coupled networks we

have presented an application to chaotic communications to transmit a train pulse as messages, from a single transmitter (node  $N_1$ ) to remote multiple receivers (nodes  $N_2$ ,  $N_3$ ,  $N_4$ , and  $N_5$ ) via public channels. We also give an example transmitting an image.



Figure 14. Recovered image message ("mime").

Transmitter node	Receiver nodes
$N_1$	$N_2, N_3, N_4$ and $N_5$
$N_2$	$N_3, N_4$ and $N_5$
$N_3$	$N_4$ and $N_5$
$N_4$	$N_5$
$N_5$	None

Table 1. Transmission scheme.

### Acknowledgments

This work was supported by the CONACYT, México under Research Grant No. 166654, and by UABC, México under Research No. 474.

### References

- [1] Muñoz-Pacheco J. M. & Tlelo-Cuautle E., Automatic synthesis of 2D-n-scrolls chaotic systems by behavioral modeling, *Journal of Applied Research and Technology*, Vol. 7, No. 1, 2009, pp.5-14
- [2] Pérez Núñez R., Measurement of Chua chaos and its applications. *Journal of Applied Research and Technology*, Vol. 6, No. 1, 2008, pp.45-53
- [3] Luo X., Small M., Danca MF. & Chen G., On a dynamical system with multiple Chaotic attractors, *Int. Journal Bifurcation and Chaos* 2007; 17(9):3235-3251.
- [4] Yujun N., Xingyuan W., Mingjun W. & Muanguang Z. A new hyperchaotic system and its circuit implementation, *Commun Nonlinear Sci Numer Simulat*, Vol. 15, 2010, pp.3518-3524
- [5] Qi Aixue, Zhang Chengliang & Wang Honggang. A switched hyperchaotic system and its FPGA circuitry implementation, *Journal of Electronics*, Vol. 28, No.3, 2011, pp.383-388
- [6] Cruz-Hernández C. & Martynyuk A.A., *Advances in chaotic dynamics with applications, Series: Stability, Oscillations, and Optimization of Systems*, Vol.4, Cambridge Scientific Publishers, 2010, pp.432
- [7] Cruz-Hernández C. & Nijmeijer H., Synchronization through filtering, *Int J Bifurct Chaos*, Vol. 10, No. 4, 2000, pp.763-775
- [8] López-Mancilla D. & Cruz-Hernández C., Output synchronization of chaotic systems: model-matching approach with application to secure communication, *Nonlinear Dyn. Syst. Theory*, Vol. 5, No. 2, 2005, pp.141-156
- [9] López-Mancilla D. & Cruz-Hernández C., Output synchronization of chaotic systems under nonvanishing perturbations, *Chaos, Solitons & Fractals*, Vol. 37, 2008, pp.1172-1186
- [10] Erjaee G.H. & Taghvatard H., Stability analysis of phase synchronization in coupled chaotic systems presented by fractional differential equations, *Nonlinear Dynamics and Systems Theory*. Vol. 2, No.2, 2011, pp.147-154

- [11] Fu S.H. & Pei L.J., Synchronization of chaotic systems by the generalized Hamiltonian systems approach. *Nonlinear Dynamics and Systems Theory*, Vol. 10, No.4, 2010, pp.387-396
- [12] Ju H. Park, Chaos synchronization of a chaotic system via nonlinear control, *Chaos, Solitons and Fractals*, Vol. 25, 2005, pp.579-584
- [13] Moez Feki, Sliding mode control and synchronization of chaotic systems with parametric uncertainties, *Chaos, Solitons and Fractals*, Vol. 41, 2009, pp.1390-1400
- [14] Nijmeijer H. & Mareels I.M.Y., An observer looks at synchronization, *IEEE Trans. Circ. Syst. I*. Vol. 44, No. 10, 1997, pp.882-890
- [15] Pecora L.M. & Carroll T.L., Synchronization in chaotic systems, *Physical Review Letters*, Vol. 64, 1990, pp.821-824
- [16] Sira-Ramírez H. & Cruz-Hernández C, Synchronization of chaotic systems: A generalized Hamiltonian systems approach, *Int J Bifurct Chaos*, Vol. 11, No. 5, 2001, pp.1381-1395
- [17] Suwat Kuntanapreeda, Chaos synchronization of unified chaotic systems via LMI, *Physics Letters A*, Vol. 373, 2009, pp.2837-2840
- [18] Cruz-Hernández C., Synchronization of time-delay Chua's oscillator with application to secure communication, *Nonlinear Dyn Syst Theory*, Vol. 4, No. 1, 2004, pp.1-13
- [19] Cruz-Hernández C., López-Mancilla D., García-Gradilla V., Serrano-Guerrero H. & Núñez-Pérez R., Experimental realization of binary signals transmission using chaos, *Journal of Circuits, Systems, and Computers*, Vol. 14, No. 3 2005, pp.453-468
- [20] Cruz-Hernández C., López-Gutiérrez R.M., Aguilar-Bustos A.Y. & Posadas-Castillo C., Communicating encrypted information based on synchronized hyperchaotic maps, *Int. J. Nonlinear Sci. Numer. Simul.*, Vol. 11, No. 5, 2010, pp.337-349
- [21] Kennedy M.P., Rovati R. & Setti G., *Chaotic electronics in telecommunications*, CRC Press, LLC, 2000
- [22] Kia Fallahi & Henry Leung. A chaos secure communication scheme based on multiplication modulation, *Commun Nonlinear Sci Numer Simulat*, Vol. 15, 2010, pp.368-383
- [23] Santo Banerjee, *Chaos Synchronization and Cryptography for Secure Communications: Applications for Encryption*, IGI Global, 2011
- [24] Serrano-Guerrero H., Cruz-Hernández C., López-Gutiérrez R.M., Posadas-Castillo C. & Inzunza-González E., Chaotic synchronization in star coupled networks of 3D CNNs and its application in communications, *Int. J. Nonlinear Sci. Numer. Sim.*, Vol. 11, No. 8, pp.571-580
- [25] Wang H., Han Z., Zhang W. & Xie Q., Chaotic synchronization and secure communication based on descriptor observer, *Nonlinear Dynamics*, Vol. 57, 2009, pp.69-73
- [26] Wang X., Xu B. & Zhang H., A multi-ary number communication system based on hyperchaotic system of 6th-order cellular neural network, *Commun Nonlinear Sci Numer Simulat*, Vol. 15, 2010, pp.124-133
- [27] Bar-Yam Y., *Dynamics of complex systems*, 1st Ed., Westview Press, 1997, pp.864
- [28] van Kooten Niekerk K. & Buhl H., *The significance of complexity: approaching a complex world through science, theology and the humanities*, Ashgate Publishing, 2004, pp.252
- [29] Strogatz S. H. & Stewart I., Coupled oscillators and biological synchronization, *Scientific American*, Vol. 269, No. 6, 1993, pp.102-109.
- [30] Acosta del Campo O.R., Cruz-Hernández C., López-Gutiérrez R.M., García-Guerrero E.E., Synchronization of modified Chua's circuits in star coupled networks, *Procs. Of the 6th International Conference on Informatics in Control, Automation and Robotics*, 2009, pp.162-167 Milan, Italy, July
- [31] Blasius B., Huppert A. & Stone L., Complex dynamics and phase synchronization in spatially extended ecological systems, *Nature*, Vol. 399, 1999, pp.354-359
- [32] Chow T.W.S., Jiu-Chao F. & Ng K.T., Chaotic network synchronization with applications to communications, *Int J. of Communication Systems*, Vol. 14, No. 2, 2001, pp.217-30
- [33] Cruz-Hernández C., López-Gutiérrez R.M., Inzunza-González E. & Cardoza-Avendaño L., 2009 Network synchronization of unified chaotic systems in master-slave coupling, *Procs. of the 3th International Conference on Complex Systems and Applications*, 2009, pp.56-60, Le Havre, Normandy, France, June

- [34] López-Gutiérrez R.M., Posadas-Castillo C., López-Mancilla D. & Cruz-Hernández C., Communicating via robust synchronization of chaotic lasers, *Chaos, Solitons & Fractals*, Vol. 41, No. 1, 2009, pp.277-285
- [35] Lu J. & Cao J., Adaptive synchronization of uncertain dynamical networks with delayed coupling, *Nonlinear Dynamics*, Vol. 53, 2008, pp.107-115
- [36] Manfeng H., Yongqing Y., Zhenyuan X., Rong Z. & Liuxiao G, Projective synchronization in drive-response dynamical networks, *Physica A*, Vol. 381, 2007. pp.457-466
- [37] Meng L., Yingying S. & Xinchu F., Complete synchronization on multi-layer center dynamical networks, *Chaos. Solitons and Fractals*, Vol. 41, 2009, pp.2584-2591
- [38] Posadas-Castillo C., Cruz-Hernández C. & López-Gutiérrez R.M., Synchronization in a network of Chua's circuits, *Procs. of 4th IASTED, International Conference on Circuits, Signals, and Systems*, 2006, pp.236-241, San Francisco, USA, November
- [39] Posadas-Castillo C., Cruz-Hernández C. & López-Gutiérrez R.M., Synchronization in arrays of chaotic neural networks, in *Lecture Notes in Artificial Intelligence: Foundations of Fuzzy Logic and Soft Computing*, P. Melin, O. Castillo, L.T. Aguilar, J. Kacprzyk and W. Pedrycz, Editors, No. 4529, Springer-Verlag, 2007, pp.743-754
- [40] Posadas-Castillo C., Cruz-Hernández C. & López-Mancilla D., Synchronization of chaotic neural networks: A generalized Hamiltonian systems approach, in *Hybrid Intelligent: Systems Analysis and Design*, O. Castillo, P. Melin, J. Kacprzyk, W. Pedrycz, Editors, Springer-Verlag, 2007. pp.59-73
- [41] Posadas-Castillo C., Cruz-Hernández C. & López-Gutiérrez R.M., Experimental realization of synchronization in complex networks with Chua's circuits like nodes, *Chaos, Solitons & Fractals*, Vol. 40, No. 4, 2007, pp.1963-1975
- [42] Posadas-Castillo C., Cruz-Hernández C. & López-Gutiérrez R.M., Synchronization in a network of chaotic solid-state Nd:YAG lasers, In *Procs. of the 17th IFAC World Congress*, 2008, pp.1565-1570, Seoul, Korea, July
- [43] Posadas-Castillo C., Cruz-Hernández C. & López-Gutiérrez R.M, Synchronization of 3D CNNs in Irregulars Array, *Procs. of the 16th Mediterranean Conference on Control and Automation Congress Center*, 2008, pp.321-325, Ajaccio, France, June
- [44] Posadas-Castillo C., Cruz-Hernández C. & López-Gutiérrez R.M. Synchronization of chaotic neural networks with delay in irregular networks, *Applied Mathematics and Computation*, Vol. 205, No. 1, 2008, pp.487-496
- [45] Wang X.F., Complex networks: Topology, dynamics and synchronization, *Int. J. Bifurct. Chaos*. Vol. 12. No. 5, 2002, pp.885-916
- [46] Wang X.F. & Chen G. Synchronization in small-world dynamical networks, *Int. J. Bifurct. Chaos.*, Vol 12, No. 1, 2002. pp.187-92
- [47] Wu C.W., Synchronization in complex networks of nonlinear dynamical systems, *World Scientific*, 2007, pp.168
- [48] Ledesma-Orozco S., Ruiz-Pinales I., García-Hernández G., et al., Hurst Parameter Estimation Using Artificial Neural Networks, *Journal of Applied Research and Technology*, Vol. 9, No.2, 2011, pp.227-241
- [49] Arab M. R; Suratgar A. A.; Martínez-Hernández V. M.; et al., Electroencephalogram Signals Processing for the Diagnosis of Petit mal and Grand mal Epilepsies Using an Artificial Neural Network, *Journal of Applied Research and Technology*, Vol. 8, No.1, 2010, pp.120-129
- [50] Werblin F., Roska T. & Chua L.O., The analogic cellular neural network as a bionic eye, *International Journal of Circuit Theory and Applications*, Vol. 23, No. 6, 1994, pp.541-569
- [51] Chua L.O. & Roska T., *Cellular Neural Networks and Visual Computing*, International Cambridge University Press, 2002, pp.412
- [52] Yang X.S. & Li Q., Horseshoe chaos in cellular neural networks, *Int. J. Bifurct. Chaos*, Vol. 16, No. 1, 2006, pp.157-161
- [53] Yang T., *Chaotic communication systems*, Nova Scientific Publishers Inc., 2001